BREAST

Diagnostic performance of dual-energy contrast-enhanced subtracted mammography in dense breasts compared to mammography alone: interobserver blind-reading analysis

Yun-Chung Cheung · Yu-Ching Lin · Yung-Liang Wan · Kee-Min Yeow · Pei-Chin Huang · Yung-Feng Lo · Hsiu-Pei Tsai · Shir-Hwa Ueng · Chee-Jen Chang

Abstract

Purpose To analyse the accuracy of dual-energy contrast-enhanced spectral mammography in dense breasts in comparison with contrast-enhanced subtracted mammography (CESM) and conventional mammography (Mx).

Materials and methods CESM cases of dense breasts with histological proof were evaluated in the present study. Four radiologists with varying experience in mammography interpretation blindly read Mx first, followed by CESM. The diagnostic profiles, consistency and learning curve were analysed statistically.

Results One hundred lesions (28 benign and 72 breast malignancies) in 89 females were analysed. Use of CESM improved the cancer diagnosis by 21.2 % in sensitivity (71.5 % to 92.7 %), by 16.1 % in specificity (51.8 % to 67.9 %) and by 19.8 % in accuracy (65.9 % to 85.8 %) compared with Mx. The interobserver diagnostic consistency was markedly higher using CESM than using Mx alone (0.6235 vs. 0.3869 using the kappa ratio). The probability of a correct prediction was elevated from 80 % to 90 % after 75 consecutive case readings.

Conclusion CESM provided additional information with consistent improvement of the cancer diagnosis in dense breasts compared to Mx alone. The prediction of the diagnosis could be improved by the interpretation of a significant number of cases in the presence of 6 % benign contrast enhancement in this study.

Key Points
- *DE-CESM improves the cancer diagnosis in dense breasts compared with mammography.*
- *DE-CESM shows greater consistency than mammography alone by interobserver blind reading.*
- *Diagnostic improvement of DE-CESM is independent of the mammographic reading experience.*

Keywords Mammography · Dual-energy contrast-enhanced spectral mammography · Contrast-enhanced subtracted mammography · Observer-blind study · Breast · Breast cancer diagnosis

Y.-C. Cheung · Y.-C. Lin · Y.-L. Wan · K.-M. Yeow · P.-C. Huang
Department of Medical Imaging and Intervention, Chang Gung Memorial Hospital, Linkuo/TaoYuan, Taiwan

Y.-C. Cheung · Y.-L. Wan · K.-M. Yeow · Y.-F. Lo · H.-P. Tsai · C.-J. Chang
Medical College, Chang Gung Memorial Hospital, Linkuo/TaoYuan, Taiwan

Y.-F. Lo · H.-P. Tsai
Department of Surgery, Chang Gung Memorial Hospital, Linkuo/TaoYuan, Taiwan

S.-H. Ueng
Department of Pathology, Chang Gung Memorial Hospital, Linkuo/TaoYuan, Taiwan

C.-J. Chang
Biostatistical Center for Clinical Research, Chang Gung Memorial Hospital, Linkuo/TaoYuan, Taiwan

Y.-C. Cheung (✉)
Department of Medical Imaging and Intervention, Chang Gung Memorial Hospital (Linkuo/TaoYuan Branches), Medical College of Chang Gung University, No 123, Dinghu Road, Guishan Township, TaoYuan County 333, Taiwan
e-mail: alex2143@ms33.hinet.net

Abbreviations

ACR	American College of Radiology
BI-RADS	Breast Imaging Reporting and Data System
CC	craniocaudal

CESM	contrast-enhanced subtracted mammography
DCIS	ductal carcinoma in situ
DE-CESM	dual-energy contrast-enhanced spectral mammography
GEE	generalised estimating equation
IDC	invasive ductal carcinoma
ILC	invasive lobular carcinoma
MLO	mediolateral oblique
Mo	molybdenum
MRI	magnetic resonance imaging
Mx	mammography
NPV	negative predictive value
PPV	positive predictive value
Rh	rhodium

Introduction

Mammography (Mx) is the current breast-imaging technique for both clinical and screening purposes. Detection of breast lesions is important for further evaluation and predicting the risk of malignancy. Classification using the Breast Imaging Reporting and Data System (BI-RADS) established by the American College of Radiology (ACR) is used for malignancy prediction for clinical communication or management [1]. The accuracy of cancer diagnosis depends directly on cancer detection; additional imaging facilitating the discovery of cancer in a patient may improve the outcome. However, additional images should ideally be interpreted by a radiologist using a technique with a high level of interobserver consistency and gradual learning curve for prediction of malignancy. Interobserver consistency and knowledge of malignancy prediction are the basis of correct mammogram interpretation.

Although mammography is widely established as an excellent modality for screening early breast cancer and has been reported to substantially reduce mortality, limitations of mammography due to the superimposition of dense breast fibroglandular tissues and lesions visible in only one view with subtle architectural distortions are recognised [2, 3]. The dense background may obscure an underlying mass, particularly in infiltrating or ill-defined hypodense or isodense lesions. Reportedly, 20–30 % of breast cancers are missed on mammograms [4, 5], as are 16.5 % of palpable breast cancers [6].

Clinically, sonography has become an indispensable breast-imaging tool. Many independent studies have also reported that supplemental screening sonography could additionally detect mammographically occult cancers in women with dense breasts, yielding a detection rate of 2.3–4.6 per 1,000 women [7–11]. Thus, sonography is believed to be superior to mammography in women with dense breasts or in young patients. However, the first-line detection of breast microcalcifications remains to be clarified. Furthermore, diagnosis by sonography has been reported to be operator dependent with low interobserver agreement, particularly for small masses and small malignancies [12]. In clinical settings, the interobserver agreement in BIRADS classification 3 and 4 sonograms was reported to be fair to low [12–14]. Optimally, breast sonography is reliable for target evaluation on palpable or suspicious lesions found by mammography.

Currently, the enhancement technique of intravenous injection of contrast medium enables better imaging of breast lesions and improves cancer detection. Enhanced breast magnetic resonance imaging (MRI) with dedicated breast coils is considered the most accurate imaging modality for cancer detection, with a sensitivity of 79–98 % [15, 16]. Similarly, the iodinated contrast medium used in computed tomography examinations showed enhancement of a hypervascular lesion with higher cancer detection than conventional mammography [17].

Recently, dual-energy contrast-enhanced spectral mammography (DE-CESM) proved to be a new breast imaging modality that encompasses the traditional low-energy Mx and provides additional contrast-enhanced subtracted mammography (CESM) using the masking technique between the low- and high-energy mammograms. The subtracted mammogram can highlight hypervascular lesions for evaluation and thus increase cancer detection. Many articles have documented the usefulness of CESM in cancer detection [18–21]. However, in clinical practice the prevalence is underestimated in certain subpopulations. For the subpopulation with dense breasts, we conducted a multi-reader blind study to evaluate the improvement of diagnosis, interobserver consistency and learning curve with additional CESM compared with Mx.

Materials and methods

Patient selection

Our institutional review board approved this retrospective study. We began using DE-CESM in 2012 after the approval by the US Food and Drug Administration in 2011. In this study, we reviewed all DE-CESM examinations performed from February 2012 to December 2012. All of the patients routinely underwent high-resolution breast sonography according to the clinical work-up. However, sonography was performed either before, after or repeated after DE-CESM. Thus, we did not compare the results of DE-CESM and sonography in this study. The clinical data of histological diagnoses and lesion locations were recorded using the Excel

software. The blind-reading study was conducted using the same order of cases to assess the test among multiple readers.

A full explanation of the advantages of the examination, the examination procedure, the contrast medium injection and the potential complications including allergic reaction to the contrast medium was provided to all participants who agreed to receive the new mammogram examination. Exclusion criteria included renal function impairment, pregnancy, lactation, a history of an allergic reaction to contrast medium and certain systemic diseases, such as hyperthyroidism. Renal function impairment was routinely evaluated by serum creatinine and glomerular filtration rate. Written informed consent for examination was obtained from each participant.

The inclusion criteria selected for the blind-reading study included a dense breast either with ACR density classification 3 or 4 according to mammography, and with lesions histologically confirmed by core-needle biopsy or surgery. Breast density was based on the clinical mammography results scored by the first author. Classification 3 referred to a heterogeneously dense breast with more than 50 % but less than 75 % opaque tissue, and classification 4 referred to an extremely dense breast with more than 75 % opaque tissues. The histological results were recorded and subdivided into benign and malignant groups for statistical analysis.

DE-CESM technique and protocol

The DE-CESM used in this study was a commercial model developed by GE Healthcare (Senographe Essential CESM, Buc, France). The mammography instrument provided intermittent exposure to low and high energy in a single breast-compressed position. All CESM acquisitions were compatible with a full-field digital mammography system. Two spectral images obtained using different energy levels were used to create a subtracted image by masking the high-energy mammogram to the low-energy mammogram. For the low-energy imaging, molybdenum (Mo) and rhodium (Rh) with Mo and Rh filters at peak voltage (kVp) values ranging from 26 to 31 were used. A Mo target with a copper-layer filter at 45 to 49 kVp was used to obtain the high-energy image. Exposure to Mo or Rh was selected depending on the breast thickness. This technical design ensures that the x-ray spectrum is below and above the k-edge of iodine (33.2 keV) for a successful CESM. Acquisition of low- and high-energy images resulted in generation of a subtracted image that indicated the presence of iodine uptake after elimination of the noise due to non-enhanced anatomic structures.

The DE-CESM was standardised. An intravenous catheter was inserted in the forearm prior to the examination. After the single-bolus injection of non-ionised contrast medium (Omnipaque 350 mg I/mL; GE Healthcare, Dublin, Ireland) via an intravenous catheter at a rate of 3 mL/s for a total dose of 1.5 mL/kg body weight, consecutive mammogram acquisitions were performed sequentially with craniocaudal (CC) and mediolateral oblique (MLO) views of the bilateral breasts. Thus, the acquisitions of CC and MLO mammograms were obtained within approximately 2–3 and 3–6 min, respectively, after contrast medium injection. In this study, the sequence of CC and MLO views was designed taking into consideration the optimal acquisition of cancer enhancement as early as possible to minimise the background influence of gradually slower enhancement of breast glandular tissues. Thus, the rapid and simple CC view was performed first. Conversely, mammograms of bilateral breasts taken at approximately similar times would facilitate comparison of the enhancement of bilateral breasts. A nurse and the mammographer were present to identify any extravasation or allergic reactions to contrast medium. The patients were requested to hold their breath during mammography exposure to avoid artefacts due to motion. Low- and high-energy acquisitions were immediately computerised and a subtracted mammogram created using the low-energy mammogram as a mask. Low-energy Mx and CESM were obtained in each single-study view. Eight mammography images from bilateral breasts were obtained per examination.

Blind-reading method and statistical analysis

The first author reported all CESM examinations in clinical terms with correlations to the clinical information and other images. Thus, the clinical results from the first author were not included in the analysis. The blinded radiologists read the cases in the same order of ascending chart number. Four radiologists with different durations of mammography-interpretation experience were asked to participate in the blind reading. They were blinded to the patients' clinical data and had no experience with CESM. However, they had experience with breast sonography and enhanced MRI; thus, they were familiar with benign enhancement, although the scale of enhancement was unknown.

The radiologists separately read the Mx (low-energy Mx) first, followed by the CESM. They were requested to identify the lesion first and then to score the malignant probability (ACR BI-RADS 1 to 5) for each mammography reading. Before making the final CESM decision, they were allowed to re-evaluate the corresponding enhanced area on Mx. The Mx and CESM therefore had two individual malignancy scores corresponding to Mx alone and Mx + CESM. If the locations of suspicious lesions and histologically confirmed lesions were discordant, an incorrect diagnosis was determined regardless of whether the malignant score was correct. After finishing each case, the histological diagnosis was revealed to the radiologists.

For statistical analysis, BI-RADS 1 to 3 and BI-RADS 4 to 5 were classified into the suspicious benign and suspicious malignant groups, respectively. In reference to the gold

standard of histological diagnosis, the rates of true positive, true negative, false positive and false negative for malignancy were counted. The diagnostic sensitivity (number of true positives/total number of lesions with histologically confirmed malignancy), specificity (number of true negatives/total number of lesions with histologically confirmed benignity), positive predictive value (PPV; number of true positives/total number of BI-RADS 4 and 5), negative predictive value (NPV; number of true negatives/total number of BI-RADS 1, 2, 3) and accuracy (number of true positives plus true negatives/total number of lesions with histological diagnoses) were defined. The blind study results were analysed statistically both per reader and across readers. The generalised estimating equation (GEE) was used to assess the significance of differences, as well as to generate a learning curve for the correct prediction of malignant probability using a logistic regression model (SPSS, version 17, Chicago, IL, USA). Otherwise, the kappa ratio was used to express the consistency of the results of the four blinded radiologists.

Results

Of 156 DE-CESM examinations reviewed, 89 patients (33–69 years of age, average 48 years) with 100 histologically confirmed lesions in dense breasts (BI-RADS density class 3 in 67 cases and class 4 in 22 cases) were enrolled. Eleven patients had bilateral breast lesions; 52 lesions were palpable and 48 were non-palpable. Among them, 21 clustered microcalcifications were diagnosed by stereotactic mammography-guided, vacuum-assisted core-needle biopsy,

while the other 79 sonographically detectable lesions were diagnosed by sonography-guided large-bore core-needle biopsy. Finally, 28 lesions were diagnosed as benign and 72 as malignant (Table 1).

When assessing the diagnostic value of enhancement, the presence of an associated enhancement was based on the clinical reports by the first author. Assuming that the enhancement indicated malignancy, the clustered microcalcifications found on mammography and sonographically detected masses were analysed individually.

All 21 clustered microcalcifications were non-palpable and did not have associated suspicious lesions on the basis of sonographic examination. However, all were diagnosed as having a risk of malignancy (BI-RADS 4 or 5). The microcalcifications were then pathologically confirmed using stereotactic mammography-guided vacuum-assisted core-needle biopsy with a 10-gauge, large-bore needle. In cases with multifocal microcalcifications, the site with associated enhancement was the first priority for biopsy.

Seven patients were diagnosed with cancer on the basis of stereotactic biopsy, and 14 patients were diagnosed with benign lesions (Table 1). In total, 9 of 21 cases revealed the presence of associated enhancement at the sites of microcalcifications on DE-CESM (Fig. 1); they were histologically diagnosed as ductal carcinoma in situ (DCIS) in three patients, invasive ductal carcinoma (IDC) in two patients, invasive lobular carcinoma (ILC) in one patient, flat epithelial atypia in two patients and nonproliferative breast disease in one patient. Overall, enhancement was documented in six breast cancers and three benign lesions.

Among the remaining 79 sonographically detectable masses, 65 lesions were histologically diagnosed as

Table 1 Histological diagnoses of 100 breast lesions

Pathological diagnoses	Isolated microcalcification	Sonography-detectable mass	Total number of lesions
Malignant lesions	7	65	72
Invasive ductal carcinoma	2	48	50
Ductal carcinoma in situ	4	10	14
Invasive mucinous carcinoma	0	3	3
Invasive lobular carcinoma	1	2	3
Adenoid cystic carcinoma	0	1	1
Angiosarcoma	0	1	1
Benign lesions	14	14	28
Flat epithelial atypia	7	0	7
Adenosis	3	4	7
Proliferative breast disease	2	1	3
Ductal hyperplasia	1	2	3
Papilloma	0	3	3
Fibroadenoma	0	3	3
Nonproliferative breast disease	1	0	1
Myoid hamartoma	0	1	1
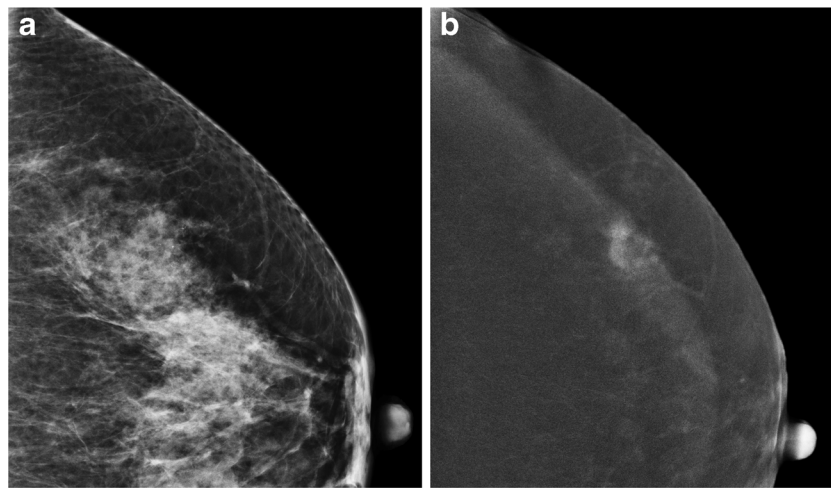
Fig. 1 A 56-year-old asymptomatic female without a detectable mass on breast sonography. **a** The CC view of conventional mammography showed a cluster of a few isolated, amorphous microcalcifications in the upper outer quadrant of the left breast. No suspicious mass was noted. **b** CESM revealed a 1.3-cm, enhanced irregular lesion associating with the isolated microcalcifications that was later proven to be invasive ductal carcinoma by both stereotactic biopsy and subsequent partial mastectomy

malignant, and 14 as benign (Table 1). Enhancement was observed in 64 malignant tumours and 3 benign lesions. The enhanced malignant lesions included 48 IDCs, 9 DCISs, 3 invasive mucinous carcinomas, 2 ILCs, 1 adenoid cystic cancer, and 1 angiosarcoma. The enhanced benign lesions included two fibroadenomas and one hamartoma.

The sensitivity, specificity, PPV, NPV and accuracy based on enhancement for the clustered microcalcifications were calculated as 85.7 % (6/7), 78.5 % (11/14), 66.6 % (6/9), 90.9 % (11/12) and 80.9 % (17/21), respectively. For cases with sonographically detected masses, the sensitivity, specificity, PPV, NPV and accuracy based on enhancement were calculated as 98.4 % (64/65), 78.5 % (11/14), 95.5 % (64/67), 90.9 % (10/11) and 94.9 % (75/79), respectively.

Blind-reading results

The sensitivity, specificity, PPV, NPV and accuracy of diagnosis by the four readers are listed in Table 2. The sensitivity, specificity, PPV, NPV and accuracy of Mx alone ranged from 59.7 % to 83.1 %, 32.1 % to 80.1 %, 74.7 % to 89.6 %, 36 % to 50 % and 61 % to 71.7 %, respectively. However, the ranges of sensitivity, specificity, PPV, NPV and accuracy by DE-CESM were comparatively narrower, from 90.2 % to 95.8 %, 57.1 % to 75 %, 85 % to 90.3 %, 75 % to 85.7 % and 84 % to 87 %, respectively. Compared with the Mx alone, the sensitivity, specificity, PPV, NPV and accuracy of the DE-CESM were improved by an average of 21.2 %, 16.1 %, 8.2 %, 37.4 % and 19.9 %, respectively (Table 3).

The diagnostic consistency among the four observers was higher in DE-CESM than Mx alone (0.6235 vs. 0.3869 by kappa ratio). The probability of a correct prediction was 80–90 % after diagnosis of 75 consecutive lesions, and reached 92.4 % after 100 lesions (Fig. 2).

Discussion

DE-CESM is a newly developed breast imaging technique for cancer detection to be used in addition to Mx. After automatic sequential low- and high-energy exposures within a short interval, two low- and high-energy mammograms are obtained from a single view. As a result of the k-edge of iodine, the two low- and high-energy mammograms should have different attenuations in the area of iodine despite being indistinguishable in the mammography images. However, the computer can analyse the differences using formulated calculations and create a subtracted image, which indicates the presence of iodine uptake. The technical and clinical experiences of using CESM in addition to conventional Mx have been published elsewhere [18–20, 22].

Similar to enhanced breast MRI, cancer detection was based on angiogenesis in the malignant tumours. Tumour enhancement was due to leakage of the contrast medium from the immature tumour vessels into the interstitial spaces. Kinetic time enhancement of malignant tumours by CESM was an interesting area of investigation. However, there was no evidence of its clinical relevance. The intra-temporal mean vascular density by CD-34 immunohistological staining and the quantitative characteristics of time enhancement kinetics were poorly correlated, even by enhanced mammography or enhanced MRI [22, 23]. However, the temporal subtraction of CESM was assessed using an approach similar to enhanced MRI [18–20]. Thus, we investigated primarily the clinical assessment of cancer diagnosis by focusing on dense breasts, which are a common problem in the clinical setting.

Dense parenchymal background on a mammogram is a problematic issue because lesions can be superimposed and hidden under opaque tissues, rendering cancer detection challenging. The reported overall sensitivity of Mx was 78 %;

Table 2 The sensitivity, specificity, PPV, NPV and accuracy of Mx alone and Mx + CESM blind readings

Readers	A (95 % CI)	B (95 % CI)	C (95 % CI)	D (95 % CI)	p
Sensitivity					
Mx	77.8	59.7	83.1	65.3	0.0001
	(66.2–86.4)	(47.5–70.9)	(71.9–90.6)	(53.1–75.9)	
Mx + CESM	94.4	90.3	95.8	90.3	0.2436
	(85.7–98.2)	(80.4–95.7)	(87.5–98.9)	(80.4–95.7)	
Specificity					
Mx	32.1	82.1	42.8	50	<0.0001
	(47.6–83.4)	(62.4–93.2)	(25.0–62.6)	(31.1–68.9)	
Mx + CESM	57.1	75	64.3	75	0.2255
	(37.4–74.9)	(54.8–88.6)	(44.1–80.7)	(54.8–88.6)	
PPV					
Mx	74.7	89.6	78.7	77	N/A
	(63.1–83.7)	(76.6–96.1)	(67.4–87.0)	(64.2–86.5)	
Mx + CESM	85	90.3	87.3	90.3	N/A
	(74.9–91.7)	(80.4–95.7)	(77.5–93.4)	(80.4–95.7)	
NPV					
Mx	36	44.2	50	35.9	N/A
	(18.7–57.4)	(30.4–58.6)	(29.6–70.4)	(21.7–52.9)	
Mx + CESM	80	75	85.7	75	N/A
	(55.7–93.4)	(54.8–88.6)	(62.6–96.2)	(54.8–88.6)	
Accuracy					
Mx	65	66	71.7	61	<0.0001
	(55.7–74.3)	(55.8–75)	(61.6–80.1)	(50.7–70.4)	
Mx + CESM	84	86	87	86	0.0429
	(75–90.3)	(77.3–91.9)	(78.4–92.6)	(77.3–91.9)	

Mx experience of readers: A= 20 years, B=12 years, C=6 years, D=2 years

PPV positive predictive value, *NPV* negative predictive value, *Mx* conventional mammography, *CESM* contrast-enhanced subtracted mammography, *N/A* not applicable

however, the sensitivity decreased from 90 % for non-dense breasts (BI-RADS 1 and 2) to 56 % for dense breasts (BI-RADS 3 and 4) [24]. In solving the interruption of superimposed breast tissues, tomosynthesis has been developed recently as a new adjunct to mammography for the interpretation of several contiguous mammographic slices. The sensitivity and specificity of breast tomosynthesis could be theoretically improved compared with two-dimensional mammography [25, 26]. A multi-reader performance study reported that the diagnostic performance of tomosynthesis was non-inferior to that of mammography [27]. However, a subsequent comparative study documented that additional tomosynthesis was non-superior to mammography and sonography [28]. Further clinical studies are needed to clarify the role of additional breast tomosynthesis in the traditional diagnostic work-up.

Table 3 Average sensitivity, specificity, PPV, NPV and accuracy of Mx and Mx + CESM

	Mx	Mx + CESM	Difference
Sensitivity	71.5	92.7	21.2
Specificity	51.8	67.9	16.1
PPV	80	88.2	8.2
NPV	41.5	78.9	37.4
Accuracy	65.9	85.8	19.9

PPV positive predictive value, *NPV* negative predictive value, *Mx* conventional mammography, *Mx + CESM* conventional mammography plus contrast-enhanced subtracted mammography
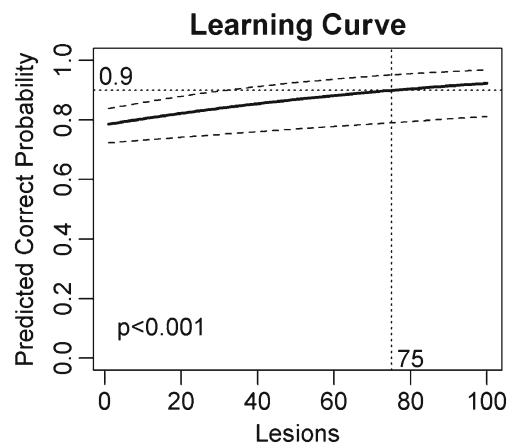
Fig. 2 The learning curve generated using the logistic regression model represents the predicted correct probability (*black line*) and 95 % confidence interval (*dotted lines*) against the number of lesions read across the four blind readers. A predicted correct probability of 90 % was achieved after reading 75 lesions (marked line at 75 lesions)
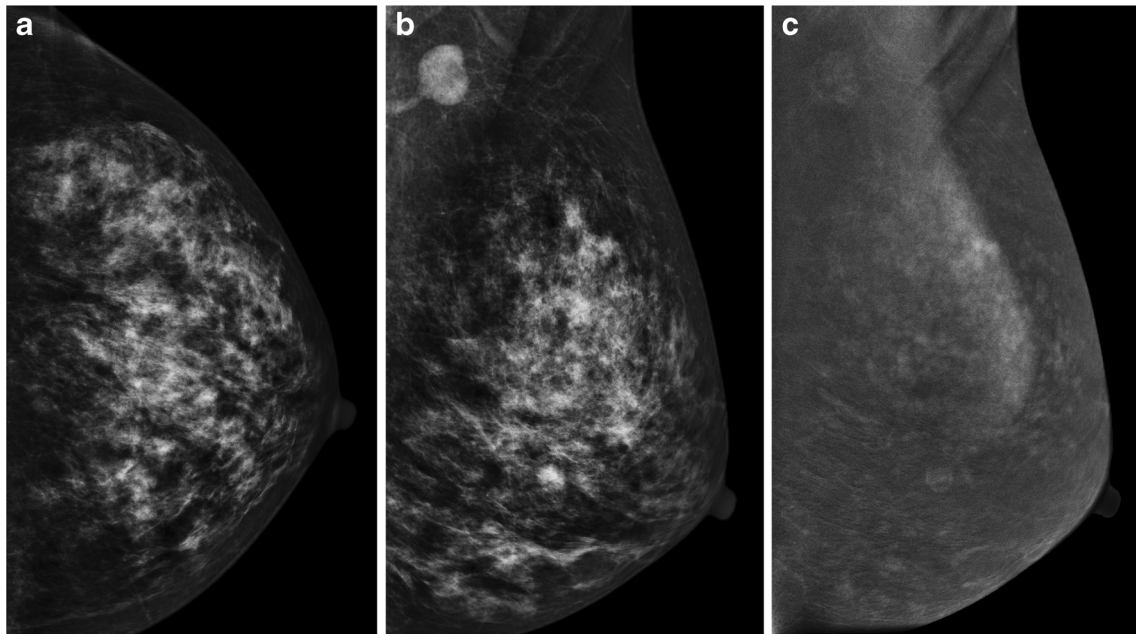
Fig. 3 A 54-year-old female with a proven metastatic axillary lymph node, but negative on initial sonography examination. **a** The CC view of the conventional mammography did not show a suspicious mass in the left breast. **b** The MLO view of conventional mammography revealed an 8-mm, smooth-outlined, hyperdense nodule in the retroareolar region of the left breast. **c** The MLO view of CESM demonstrated target enhancement of the nodule. Repeated sonography subsequently proved the nodule to be invasive ductal carcinoma by needle biopsy

Regarding DE-CESM, the technique is different to breast tomosynthesis although both methods are mammography-based. DE-CESM could provide information additional to that provided by conventional mammography and so facilitate detection or differential diagnosis, as illustrated by the following cases of small-sized malignant tumours (Fig. 3), and isodense (Fig. 4), hypodense (Fig. 5) or cystic malignant tumours (Fig. 6) or certain benign hypervascular lesions (Fig. 7). However, CESM could faithfully diagnose a lesion that was visible in only one view of conventional mammogram (Fig. 3).
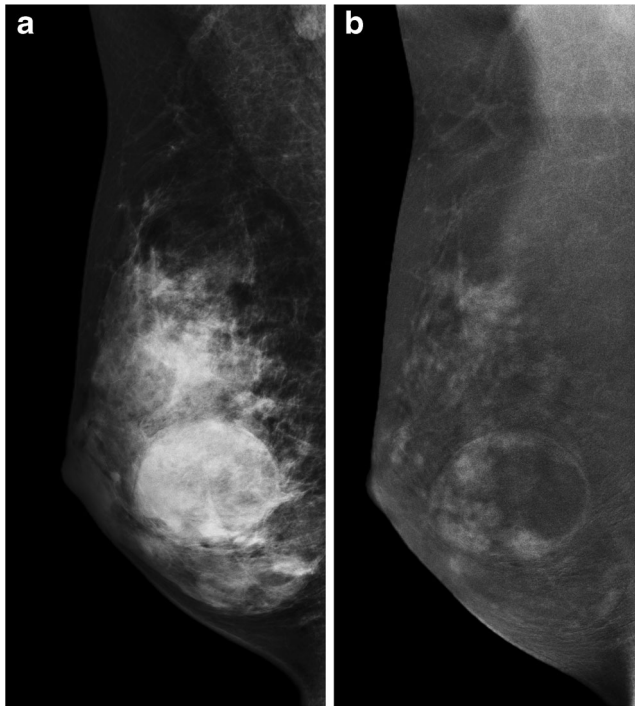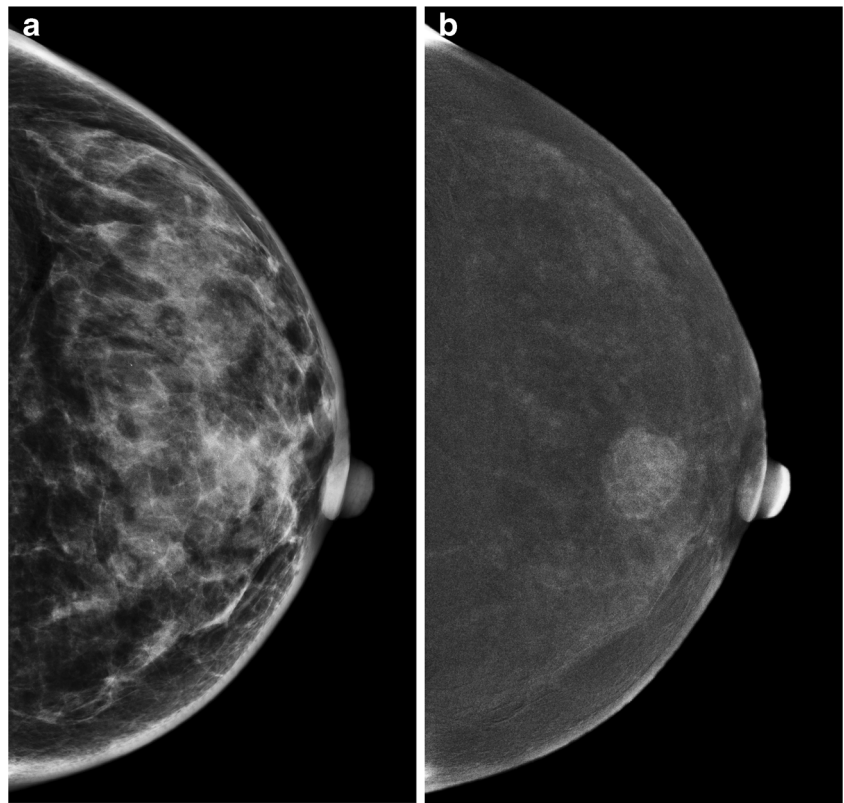
Conventional mammography and breast high-resolution sonography are the basic routine breast clinical examination methods. Many studies have published the results of addition of CESM to Mx, either with or without sonography. When comparing the addition of CESM to mammography alone, a study of a reader with CESM experience showed a significant improvement in sensitivity compared with the initial clinical result. Using BI-RADS scoring, the sensitivity and performance improved by 15 % (78 % to 93 %) and 17 % (74 % to 91 %), respectively. The specificity also increased by 5 % (58 % to 63 %) [13]. Another multi-reader study compared Mx + CESM + sonography to Mx + sonography and reported a significant improvement, with the sensitivity increasing from 71 % to 78 % and clinical performance from 83 % to 87 % [29].

In a dense breast study involving three readers with mammography interpretation experience ranging from 8 to 10 years, the sensitivity improved from 35 % to 59 % with
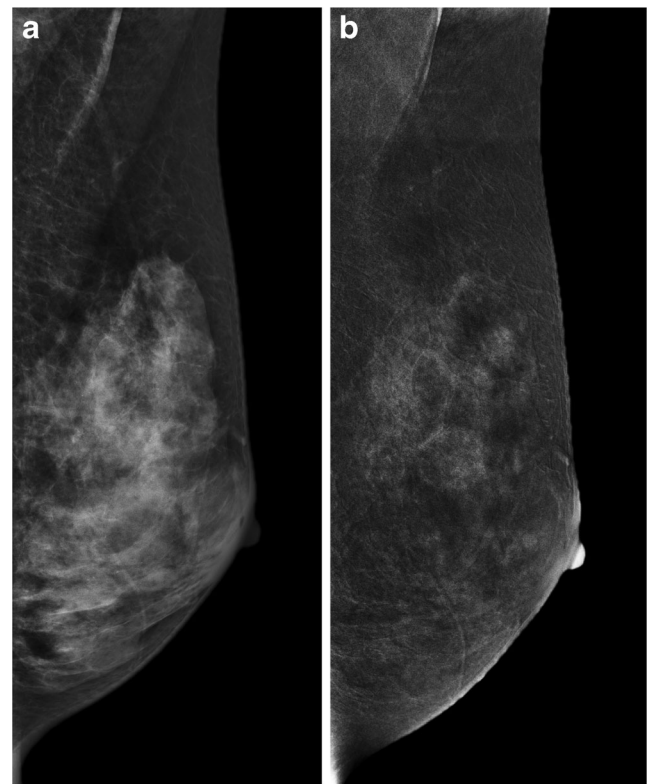
Fig. 4 A 44-year-old female with a soft palpable mass that was suspected to be a fibrocystic lump and had been followed up as a stationary mass for 6 months by sonography. **a** The MLO view of conventional mammography showed an isodense lump over the upper region of the left breast. **b** CESM demonstrated a 4-cm, irregular mass lesion with an infiltrating and a nodular architectural appearance. The lesion was finally proven to be invasive ductal carcinoma

Fig. 5 A 39-year-old female with a palpable mass in the subareolar region of the left breast. **a** The CC view of conventional mammography did not reveal the mass. **b** CESM displayed a spherical mass with honeycomb enhancement. The tumour was finally proven to be invasive ductal carcinoma


Fig. 6 A 43-year-old female with a palpable mass in her right breast. **a** The MLO view of conventional mammography showed a 4.5-cm, oval, opaque mass with a smooth outline in the lower region of the right breast. **b** CESM demonstrated the mass to have thick capsular enhancement with multiple enhanced, soft-tissue components. The mass was finally histologically diagnosed as invasive mucinous carcinoma

CESM, while the specificity decreased slightly from 69 % to 62 % [30]. However, the sensitivity in our study improved from 71.5 % to 92.7 % and the specificity from 51.8 % to 67.9 %. Different application of CESM may explain the different outcomes. The images were created by subtracting the post-contrast to the pre-contrast mammogram in a single view of a fixed position, which was completely different to the procedure used in this study. The unilateral breast was examined in only a single session. When using the DE-CESM, bilateral breasts were examined in a session during which both traditional craniocaudal and mediolateral oblique views were obtained. This implies that a two-view assessment is superior to a one-view assessment. The contrast medium distributed via blood flow to the breasts was not interrupted by breast compression, and the enhancement could be evaluated by comparison with the bilateral mammogram; these are advantages of the DE-CESM.

Dense breasts containing abundant glandular tissues might be enhanced owing to fibrocystic change and adenosis. On the basis of the MRI Lexicon, the fibrocystic breast is occasionally enhanced as a non-mass patch, typically symmetrical in bilateral breasts or adenosis as numerous homogeneous, mild-enhanced nodules (usually with uniform size around 5 mm) evenly distributed in the breasts unilaterally or bilaterally [31]. However, the individual diagnosis may still be incorrect. Diagnostic consistency, i.e. whether the diagnosis outcome

Fig. 7 A 54-year-old female with proven right palpable breast cancer received DE-CESM for pre-operative evaluation. **a** The CC view of conventional mammography showed a calcified fibroadenoma in the left breast. **b** CESM enhanced another 1.1-cm mass at left subareolar region that was not observed on the conventional mammogram and initial sonography, but was detectable on the repeated sonography. The mass was finally histologically diagnosed to fibroadenoma
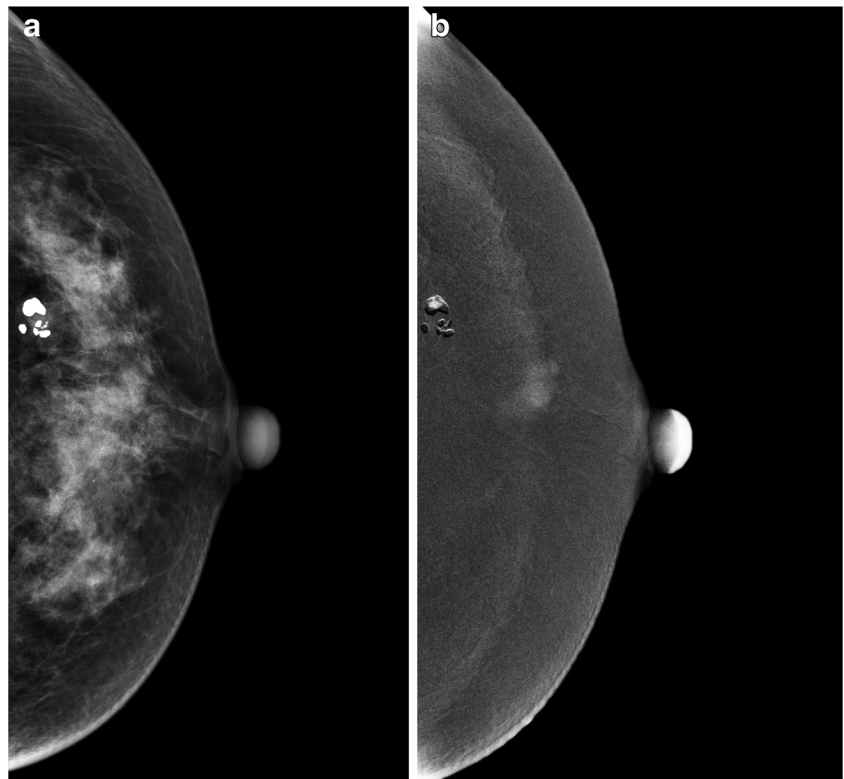
independently varied among the experiences, was an additional concern. Our blind multi-reader study showed that the consistency of CESM was significantly higher than that of Mx (kappa ratio 0.6235 vs. 0.3869 per BI-RADS) across the four readers with varying experience. Our results showed improvement compared with another multi-reader CESM study that also used a single view (kappa ratio 0.416 for malignancy) [30].

The identification of enhancement on CESM is a priority for cancer diagnosis. The morphology, intensity or time of enhancement could indicate differentiation. According to DE-CESM, masses with an irregular or lobular outline or shape, stronger enhancement or presence of associated suspicious malignant microcalcification should be considered as malignancies. The protocol design is therefore important for identification of lesions at the appropriate time, such as the early phase on CC view (within 2–3 min after contrast medium injection) and later phase on MLO view (3–7 min after contrast medium injection) as in the author's protocol. A standardised protocol could provide a timetable for lesion enhancement, which would facilitate differentiation of a lesion from adenosis or breast tissue enhancement. Comparing bilateral breast parenchymal enhancement, particularly in dense breasts, can be an important process in mammogram interpretation.

In this study, we evaluated the probability of correct prediction, as well as the representative learning curve among the blinded radiologists. The correct prediction curve showed a steady increase from 80 % to 92.4 % after diagnosing 100 lesions. Apparently, CESM technique was easily learned which may be attributed to the basic mammography observations.

In conclusion, DE-CESM provided additional information compared with Mx, with consistent improvement of cancer diagnosis in dense breasts. The observers with different level of expertise in Mx could improve their sensitivity, specificity, PPV, NPV and accuracy when using DE-CESM instead of Mx alone. The accuracy among observers was statistically significant with an error probability lower than 0.05. Otherwise, the prediction of diagnosis could be improved by the interpretation of a significant number of cases in the presence of 6 % benign contrast enhancement in this study.

References

1. American College of Radiology (2003) Breast imaging reporting and data system: BI-RADS, 4th edn. American College of Radiology, Reston

2. Humphrey LL, Helfand M, Chan BK et al (2002) Breast cancer screening: a summary of the evidence for the US Preventive Services Task Force. Ann Intern Med 137:347–360

3. Rosenberg RD, Hunt WC, Williamson MR et al (1998) Effects of age, breast density, ethnicity, and estrogen replacement therapy on screening mammographic sensitivity and cancer stage at diagnosis: review of 183,134 screening mammograms in Albuquerque, New Mexico. Radiology 209:511–518

4. Pisano ED, Gatsonis C, Hendrick E et al (2005) Digital Mammographic Imaging Screening Trial (DMIST) Investigators Group. Diagnostic performance of digital mammography versus film mammography for breast-cancer screening. N Engl J Med 353: 1773–1783

5. Holland R, Mravunac M, Hendriks JH et al (1982) So-called interval cancers of the breast: pathologic and radiologic analysis of sixty-four cases. Cancer 49:2527–2533

6. Coveney EC, Geraghty JG, O'Laoide R et al (1994) Reasons underlying negative mammography in patients with palpable breast cancer. Clin Radiol 49:123–125

7. Crystal P, Strano SD, Shcharynski S et al (2003) Using sonography to screen women with mammographically dense breasts. AJR Am J Roentgenol 181:177–182

8. Kaplan SS (2001) Clinical utility of bilateral whole-breast US in the evaluation of women with dense breast tissue. Radiology 221:641–649

9. Hooley RJ, Greenberg KL, Stackhouse RM et al (2012) Screening US in patients with mammographically dense breasts: initial experience with Connecticut Public Act 09-41. Radiology 265:59–69

10. Leconte I, Feger C, Galant C et al (2003) Mammography and subsequent whole-breast sonography of nonpalpable breast cancers: the importance of radiologic breast density. AJR Am J Roentgenol 180:1675–1679

11. Corsetti V, Houssami N, Ferrari A et al (2008) Breast screening with ultrasound in women with mammography-negative dense breasts: evidence on incremental cancer detection and false positives, and associated cost. Eur J Cancer 44:539–544

12. Abdullah N, Mesurolle B, El-Khoury M et al (2009) Breast imaging reporting and data system lexicon for US: interobserver agreement for assessment of breast masses. Radiology 252:665–672

13. Raza S, Chikarmane SA, Neilsen SS et al (2008) BI-RADS 3, 4, and 5 lesions: value of US in management—follow-up and outcome. Radiology 248:773–781

14. Heinig J, Witteler R, Schmitz R et al (2008) Accuracy of classification of breast ultrasound findings based on criteria used for BI-RADS. Ultrasound Obstet Gynecol 32:573–578

15. Morris EA, Liberman L, Ballon DJ et al (2003) MRI of occult breast carcinoma in a high- risk population. AJR Am J Roentgenol 181: 619–626

16. Berg WA (2003) Rationale for a trial of screening breast ultrasound: American College of Radiology Imaging Network (ACRIN) 6666. AJR Am J Roentgenol 180:1225–1228

17. Prionas ND, Lindfors KK, Ray S et al (2010) Contrast-enhanced dedicated breast CT: initial clinical experience. Radiology 256:714–723

18. Jong RA, Yaffe MJ, Skarpathiotakis M et al (2003) Contrast-enhanced digital mammography: initial clinical experience. Radiology 228:842–850

19. Diekmann F, Diekmann S, Jeunehomme F et al (2005) Digital mammography using iodine-based contrast media: initial clinical experience with dynamic contrast medium enhancement. Invest Radiol 40:397–404

20. Dromain C, Balleyguier C, Muller S et al (2006) Evaluation of tumor angiogenesis of breast carcinoma using contrast enhanced digital mammography. AJR Am J Roentgenol 187:W528–W537

21. Dromain C, Thibault F, Muller S et al (2011) Dual-energy contrast-enhanced digital mammography: initial clinical results. Eur Radiol 21:565–574

22. Lewin JM, Isaacs PK, Vance V et al (2003) Dual-energy contrast-enhanced digital subtraction mammography: feasibility. Radiology 229:261–268

23. Su MY, Cheung YC, Fruehauf JP et al (2003) Correlation of dynamic contrast enhancement MRI parameters with microvessel density and VEGF for assessment of angiogenesis in breast cancer. J Magn Reson Imaging 18:467–477

24. Kolb TM, Lichy J, Newhiuse JH (2002) Comparison of the performance of screening mammography, physical examination, and breast US and evaluation of factors that influence them: an analysis of 27,825 patient evaluations. Radiology 225:165–175

25. Dromain C, Thibault F, Diekmann F et al (2012) Dual-energy contrast-enhanced digital mammography: initial clinical results of a multireader, multicase study. Breast Cancer Res 14:R94

26. Kopans DB (2014) Digital breast tomosynthesis from concept to clinical care. AJR Am J Roentgenol 202:299–308

27. Gennaro G, Hendrick RE, Toledano A et al (2013) Combination of one-view digital breast tomosynthesis with one-view digital mammography versus standard two-view digital mammography: per lesion analysis. Eur Radiol 23:2087–2094

28. Gennaro G, Hendrick RE, Ruppel P et al (2013) Performance comparison of single-view digital breast tomosynthesis plus single-view mammography with two-view digital mammography. Eur Radiol 23: 664–672

29. Thibault F, Dromain C, Breucq C et al (2013) Digital breast tomosynthesis versus mammography and breast ultrasound: a multireader performance. Eur Radiol 23:2441–2449

30. Diekmann F, Freyer M, Diekmann S et al (2011) Evaluation of contrast-enhanced digital mammography. Eur J Radiol 78: 112–121

31. Liberman L, Mason G, Morris EA et al (2006) Does size matter? Positive predictive value of MRI-detected breast lesions as a function of lesion size. AJR Am J Roentgenol 186:426–430